Journal of the Serbian Chemical Society
JSCS@tmf.bg.ac.rs • www.shd.org.rs/JSCS
J. Serb. Chem. Soc. *89* (9) S278–S284 (2024) *Supplementary material*

SUPPLEMENTARY MATERIAL TO

Investigation of the adsorption behaviors of thymol blue, crystal violet, and rhodamine b on lichen-derived activated carbon

HÜLYA KOYUNCU[1]* and ALİ RIZA KUL[2]

[1]*Bursa Technical University, Faculty of Engineering and Natural Sciences, Chemical Engineering Department, 16310, Bursa, Turkiye and* [2]*Van Yüzüncü Yıl University, Faculty of Science, Chemistry Department, 65080, Van, Turkiye*

J. Serb. Chem. Soc. *89* (9) (2024) 1211–1226

Table S-I. Some specifications of TB, CV, and RB

	Thymol Blue	Crystal Violet	Rhodamine B
Molecular structure	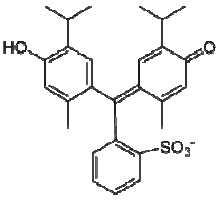	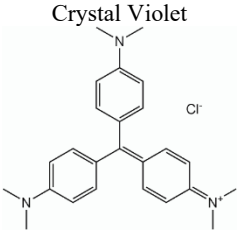	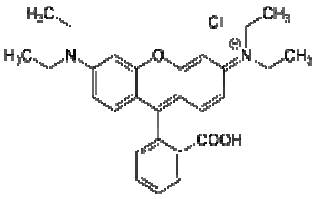
Chemical formula	C27H30O5S	C25H30ClN3	C28H31ClN2O3
Molecular weight	466.59 g/mol	407.99 g/mol	479.02 g/mol
GHS pictograms			

* Corresponding author. E-mail: hulya.koyuncu@btu.edu.tr

(a) (b)

Fig. S-1. a) Lichen *Pseudevernia furfuracea* from Ericek-Bursa; b) lichen-derived activated carbon.

Table S-II. The linearized versions of the PFO, PSO, IDM, Langmuir, Freundlich, and D-R models

Model Name	Model Equation	Plots axis (y ; x)	Model Parameter
PFO	$\ln(q_e - q_t) = \ln(q_e) - k_1 * t$	$\ln(q_e - q_t)$; t	q_e, q_t : (mg g^{-1}) k_1: (min^{-1})
PSO	$\frac{t}{q_t} = \frac{1}{k_2 * q_e^2} + \frac{t}{q_e}$ $k_0 = k_2 * q_e^2$	$\frac{t}{q_t}$; t	k_2, k_0: (g mg^{-1} min^{-1})
IDM	$q_t = k_{id} * t^{1/2} + \theta$	q_t ; $t^{1/2}$	k_d: (mg g^{-1} $min^{-1/2}$) θ: (mg g^{-1})
Langmuir	$\frac{1}{q_e} = \frac{1}{K * C_e * q_m} + \frac{1}{q_m}$	$\frac{1}{q_e}$; $\frac{1}{C_e}$	K : (L mg^{-1}) C_e: (mg L^{-1}) q_m: (mg g^{-1})
Freundlich	$\ln(q_e) = \ln(k_f) + \frac{1}{n} * \ln(C_e)$	$\ln(q_e)$; $\ln(C_e)$	k_f: (mg g^{-1})
D-R	$\ln(q_e) = \ln(q_m) - K' * \varepsilon^2$ $\varepsilon = R * T * \ln(1 + 1/C_e)$ $E = 1/\sqrt{2 * K'}$	$\ln(q_e)$; ε^2	q_m, q_e: (mol g^{-1}) ε: Polanyi potential K': (mol^2 kJ^{-2}) E: (kJ mol^{-1})

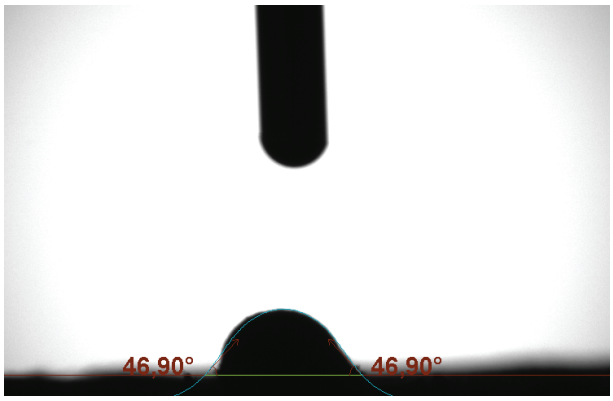

Fig. S-2. Contact angle of the LDAC.

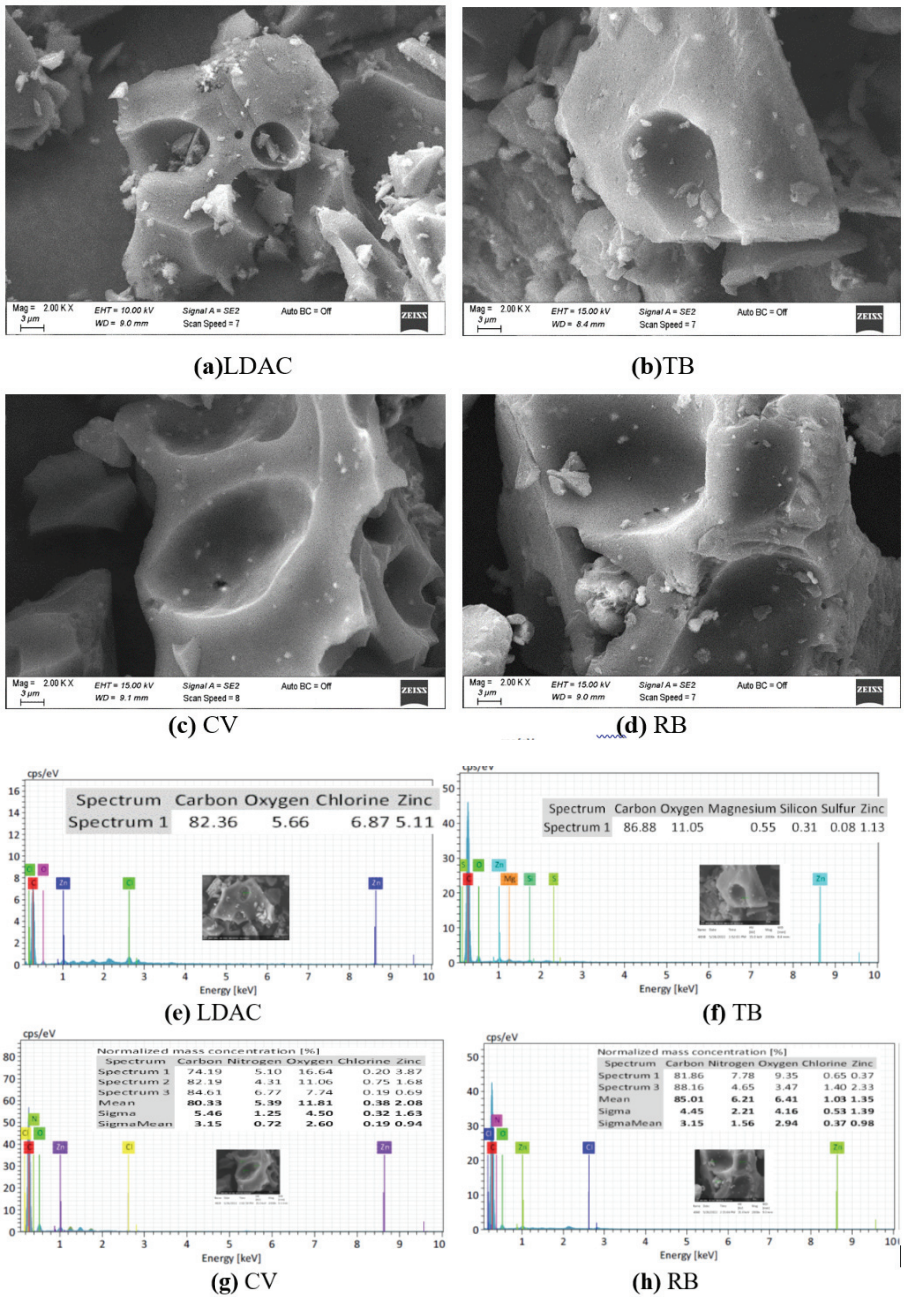

Fig. S-3. SEM photos and EDX results of the LDAC before (a, e) and after TB (b, f), CV (c, g), RB (d, h) loaded.

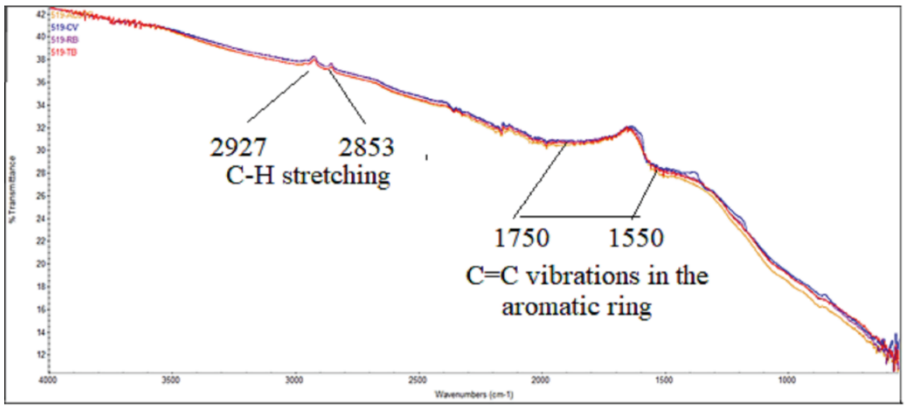

Fig. S-4. FT-IR interferograms of the LDAC before and after TB, CV, and RB loaded.

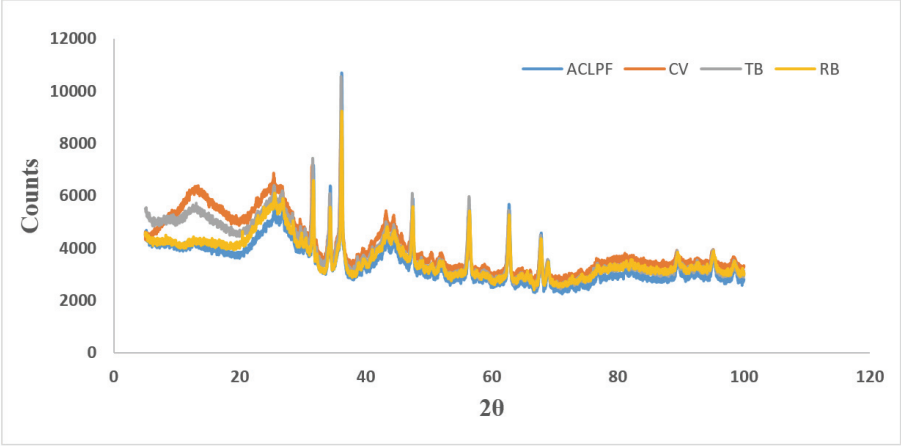

Fig. S-5. XRD patterns of the LDAC before and after TB, CV, and RB adsorptions.

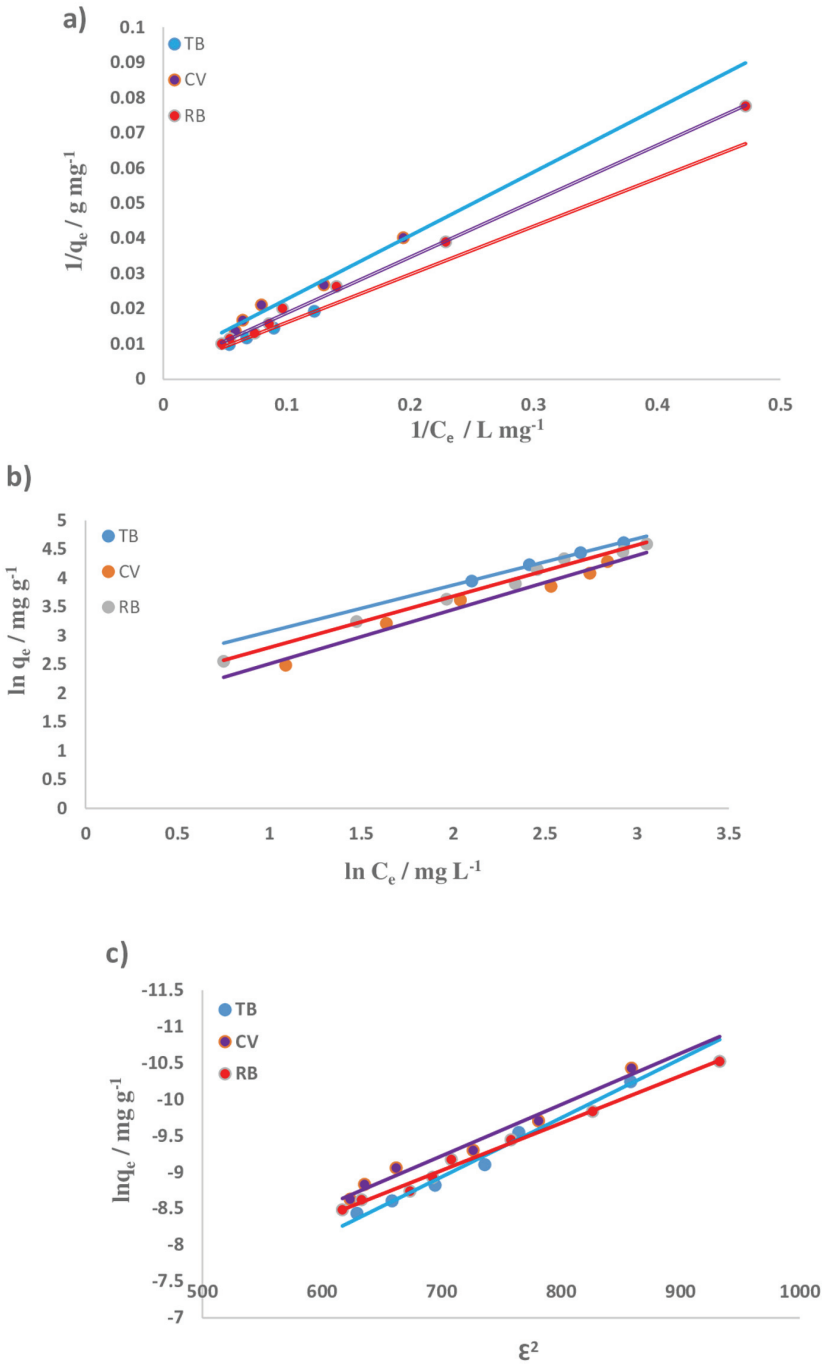

Fig. S-6. a) Langmuir; b) Freundlich; c) D-R isotherms for TB, CV, and RB.

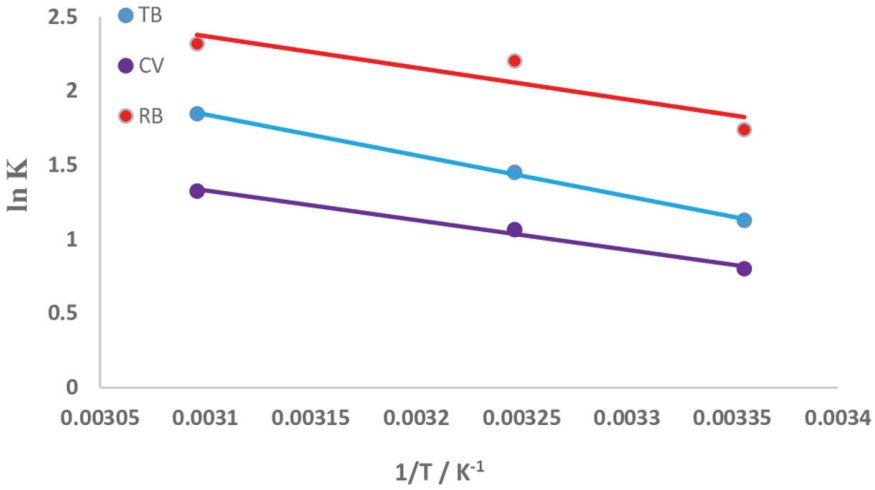

Fig. S-7. The thermodynamic plots for TB, CV, and RB adsorption.

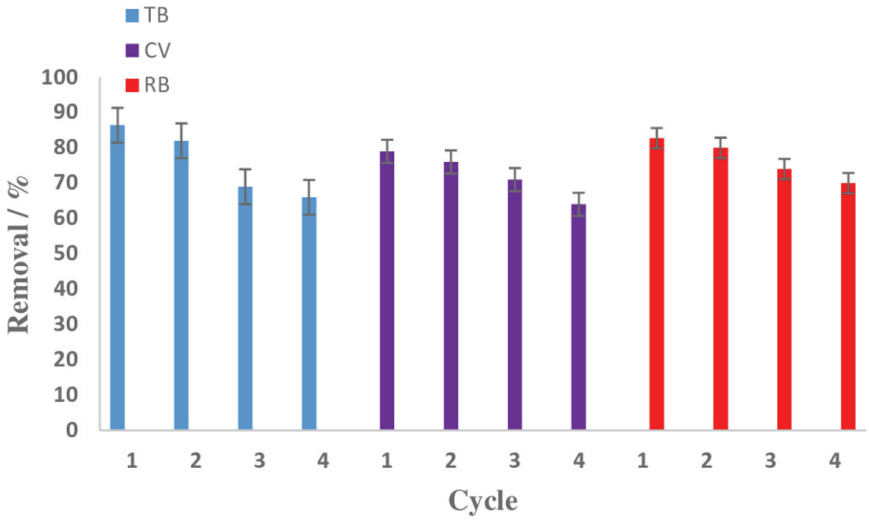

Fig. S-8. The Reusability of the LDAC for TB, CV, and RB adsorption.